DØ note 5739-CONF

Search for the Standard Model Higgs boson in the $t\bar{t}H \to t\bar{t}b\bar{b}$ channel

The DØ Collaboration
(Dated: March 14, 2009)

We present a search for the Standard Model Higgs boson produced in association with top anti-top quark pairs. This analysis considers samples of lepton+jets events with one, two or three b-tagged jets and four, five or more jets in total collected with the DØ detector, corresponding to an integrated luminosity of 2.1 fb^{-1}. Kinematical differences between $t\bar{t}$ and $t\bar{t}H$ events are exploited and limits are set on the $t\bar{t}H \to t\bar{t}b\bar{b}$ production cross section. An enhanced production cross section can theoretically be achieved if a t' quark is produced via a heavy G' boson (vector color octet) instead via a Standard Model gluon. An example for such a model is analysed here leading to an exclusion for Higgs masses below 133 GeV for a G' mass of 800 GeV and a t' mass of 400 GeV.

Preliminary Results for Summer 2008 Conferences, updated for Winter 2009 Conferences

I. INTRODUCTION

The large mass of the top quark, 172.6 ± 1.4 GeV [1], suggests that it may play an important role in the electroweak symmetry breaking scenario of the Standard Model (SM). In the SM it is predicted that the top quark has a Yukawa coupling to the Higgs boson of order unity. The production of a Higgs boson in association with a top-antitop quark pair allows the study of the top Yukawa coupling which plays a key role in understanding the nature of mass generation. It is interesting to note that if a low mass Higgs boson escapes detection at the Tevatron, this channel is the most important one to study Yukawa couplings at the LHC.

In this analysis we search for such a process with the Higgs boson decaying into a bottom-antibottom quark pair, such that we have a $t\bar{t}b\bar{b}$ final state. The predicted cross section times branching ratio for the Higgs radiation off top quarks is low so that a discovery of the SM Higgs boson in this channel alone is not feasible at the Tevatron. However, it is interesting to analyse this channel because it will contribute to the combination of the SM Higgs searches at the Tevatron, especially at low Higgs boson masses. Furthermore, for the first time final states with 3 tagged b-jets and 4 or 5 jets were looked at separately. It is thus interesting to search for any deviations from the SM in those channels. For example, in Supersymmetric Two-Higgs-Doublet Models (2HDM) or in the Minimal Supersymmetric Standard Model (MSSM) at low $\tan\beta$ [2] these channels could be enhanced where $\tan\beta$ is the ratio of the real vacuum expectation values of the two Higgs doublets and $0 \leq \beta \leq \pi/2$. Furthermore there could exist anomalous contributions to the top-Yukawa coupling [3]. An enhancement of $t\bar{t}H$ production could also be given by the SM plus a new $Q = 2/3$ quark singlet T [4].

The major background to $t\bar{t}H$ production is $t\bar{t}$ production itself with addional light and b-jet production. Other backgrounds are W+jets and multijet production, which are also major backgrounds to $t\bar{t}$ production. To enhance the $t\bar{t}H$ signal we make use of the fact that $t\bar{t}H$ events with $t\bar{t}$ decaying into a lepton and jets is expected to have both a larger number of jets originating from the hadronization of six quarks as opposed to four in the $t\bar{t}$ decay, and a larger number of b-tagged jets due to two additional b quarks from the Higgs decay.

We use the shapes of the H_T distributions, where H_T is defined as the scalar sum of the transverse momenta p_T of the 4 or 5 leading jets, for samples with different numbers of jets, number of b-tagged jets, and lepton type to distinguish signal and background. We also present an alternative method not using kinematical information but performing a simultaneous fit of the $t\bar{t}$ and $t\bar{t}H$ cross sections in the different channels, as described in Section VIII. The sensitivity of the method using kinematical information is $\approx 10\%$ better.

Limits are extracted using the modified frequentist CL_s approach with Poisson log-likelihood ratio test implemented as described in [5].

II. DØ DETECTOR

The DØ detector [6] includes a tracking system, calorimeters, and a muon spectrometer [7]. The tracking system consists of a silicon microstrip tracker (SMT) and a central fiber tracker (CFT), both located inside a 2 T superconducting solenoid. The tracker design provides efficient charged particle measurements in the pseudorapidity [8] region $|\eta| < 3$. The SMT strip pitch of 50–80 μm allows a precise reconstruction of the primary interaction vertex (PV) and an accurate determination of the impact parameter of a track relative to the PV [9], which are the key components of the lifetime-based b-jet tagging algorithms. The calorimeter consists of a central section (CC) covering $|\eta| < 1.1$, and two end calorimeters (EC) extending the coverage to $|\eta| \approx 4.2$. The muon system surrounds the calorimeter and consists of three layers of tracking detectors and two layers of scintillators [10]. A 1.8 T iron toroidal magnet is located outside the innermost layer of the muon detector. The luminosity is calculated from the rate for $p\bar{p}$ inelastic collisions detected using plastic scintillator arrays placed in the front of the EC cryostats.

III. EVENT SELECTION

We seek events in which a Higgs boson is radiated from a top or anti-top quark, with Higgs decaying into $b\bar{b}$. Almost every top quark decays into a W boson and a b quark. We select the $t\bar{t}$ decays in which one W boson decays to two quarks and the other to an electron or muon and a neutrino. Thus the process yields a lepton, missing E_T, four b-jets and two light quark jets. We select a data sample enriched in $t\bar{t}$ events by requiring either a lepton and jets or a single lepton at the trigger level. We further require ≥ 4 jets with transverse momentum $p_T > 20$ GeV and pseudorapidity $|\eta| < 2.5$, one isolated electron (muon) with $p_T > 20$ GeV and $|\eta| < 1.1$ ($|\eta| < 2.0$), and missing transverse energy $\not\!\!E_T > 20$ GeV (e+jets) or $\not\!\!E_T > 25$ GeV (μ+jets). The leading jet p_T is required to exceed 40 GeV. To improve the signal to background ratio at least one identified b-jet is required. More details on the event selection in the different channels and the composition of the relevant background can be found in Refs. [11, 12].

The $t\bar{t}H$ samples were generated using PYTHIA versions v6.319 and v6.409 [13]. The factorization scale was set to $Q^2 = (m_{top} + m_H/2)^2$ and the CTEQ6L1 PDF was used [14]. To evaluate the dependence of the signal acceptance on the Higgs mass, $t\bar{t}H$ samples were generated at Higgs masses of 105, 115, 125, 135, 145 and 155 GeV.

The main background to $t\bar{t}H$ production in high multiplicity b-tag bins arises from the $t\bar{t}$ process itself. The samples for $t\bar{t}$ production used in the analysis were generated using both PYTHIA v6.323 [13] and the ALPGEN 2.11 [15] leading-order event generator for the multi-parton matrix element calculation and PYTHIA for subsequent parton showering and hadronization. The factorization scale was set to $Q^2 = m_{top}^2 + \sum p_T^2(\text{jets})$ and the top quark mass is taken to be 175 GeV. Since we found differences between the generation of the $t\bar{t}b\bar{b}$ production between [15] and [13] we assign a conservative 50% systematic uncertainty to this process.

In the channel with ≥ 5 jets and ≥ 3 b-jets, the contribution due to $t\bar{t}b\bar{b}$ due to additional gluon radiation with a subsequent $b\bar{b}$ splitting is approximately 10% relative to the whole amount of $t\bar{t}$ production [15]. We have checked that $t\bar{t}b\bar{b}$ production via additional Z boson radiation with a subsequent $b\bar{b}$ splitting is smaller than 0.5% relative to the whole amount of $t\bar{t}$ production. It is thus neglected here. Other backgrounds are due to W+jets and multijet production.

All events were passed through a full DØ detector simulation and were overlaid with zero-bias data events to simulate additional interactions in the same beam crossing.

IV. SEPARATION OF SIGNAL FROM BACKGROUND

We performed studies to compare the event kinematics of W+jets, multijet and $t\bar{t}$ background events with the $t\bar{t}H$ signal in order to find variables with discrimination power between signal and background. For this purpose, samples were generated containing events with at least 4 jets. Figs. 1 and 2 show distributions of H_T, the number of jets and the number of b-tagged jets for W+jets, multijet, $t\bar{t}$ and $t\bar{t}H$ simulated events. These variables gave the greatest separation power between signal and background. We found even better separation power than for example for the invariant dijet masses. We define subsamples with 4 or ≥ 5 jets, with 1, 2 or ≥ 3 b-tags, and for the e+jets and μ+jets final states, and split the H_T distribution for each of those 12 channels into 8 bins each. Although the $t\bar{t}H$ contribution is small for events with 1 or 2 b-tags these bins help to constrain the $t\bar{t}$ background and thus improve the sensitivity by $\approx 15\%$.

Fig. 3 shows the H_T distributions for all channels with 4 or ≥ 5 jets and 1, 2 or ≥ 3 b-tagging for the full data set of 2.1 fb^{-1}. The data are compared to the different sources of background. The contribution of the $t\bar{t}H$ signal for a Higgs boson mass of 105 GeV is multiplied by 100 and overlaid (solid black histogram).

V. EVENT YIELDS AND LIMIT SETTING

The expected and observed numbers of events in the different channels are summarized in Table 1. The yields are shown for a SM Higgs boson of mass 105 GeV. The $t\bar{t}$ contribution is calculated for a theoretical $t\bar{t}$ cross section of $\sigma_{t\bar{t}} = 7.3$ pb [16, 17] for a top quark mass of 172.6 GeV which corresponds to the world average value [1].

In all channels the number of candidate events is consistent with the background expectation within the statistical and systematical uncertainties. This is interesting because we looked at the ≥ 3 b-tag channels for the first time separately. As an example, in Fig. 9 we show the display of one of the 5 events found in the channel with ≥ 5 jets and ≥ 3 b-tags. Since there is no evidence for SM $t\bar{t}H$ production we set 95% C.L. limits on the production cross section times branching ratio $\sigma(t\bar{t}H) \times B(H \to b\bar{b})$. As input for the limit calculation we use the 8 bin H_T distributions.

To set limits on the SM Higgs boson production cross section, a modified frequentist approach [18] was used, where the signal confidence level CL_s, defined as the ratio of the confidence level for the signal-plus-background hypothesis to the background-only hypothesis ($CL_s = CL_{s+b}/CL_b$), is calculated by integration of the distributions of a test statistic over the outcomes of pseudo-experiments, generated according to Poisson statistics, for the signal+background and background-only hypotheses. The test statistic is calculated as a joint log-likelihood ratio (LLR) obtained by summing LLR values over the bins of the H_T distributions. Systematic uncertainties were incorporated via Gaussian smearing of the Poisson probability distributions for signal and backgrounds within the pseudo-experiments. All correlations between signal and backgrounds were maintained. To reduce the impact of systematic uncertainties on the sensitivity of the analysis, the individual signal and background contributions were fitted to the data (and pseudo-data). This

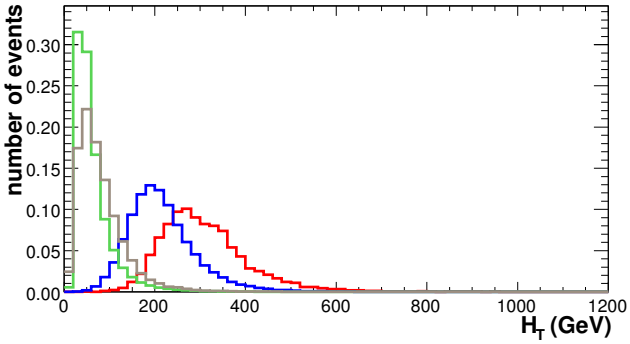

FIG. 1: Normalized distribution of H_T (applying a $p_t^{jet} > 15$ GeV cut) for $t\bar{t}H$ where the Higgs mass was set to 115 GeV (red), $t\bar{t}$ (blue), W+jets (green) and multijet (brown) production. H_T is defined as the scalar sum of the transverse momenta of the 4 leading jets.

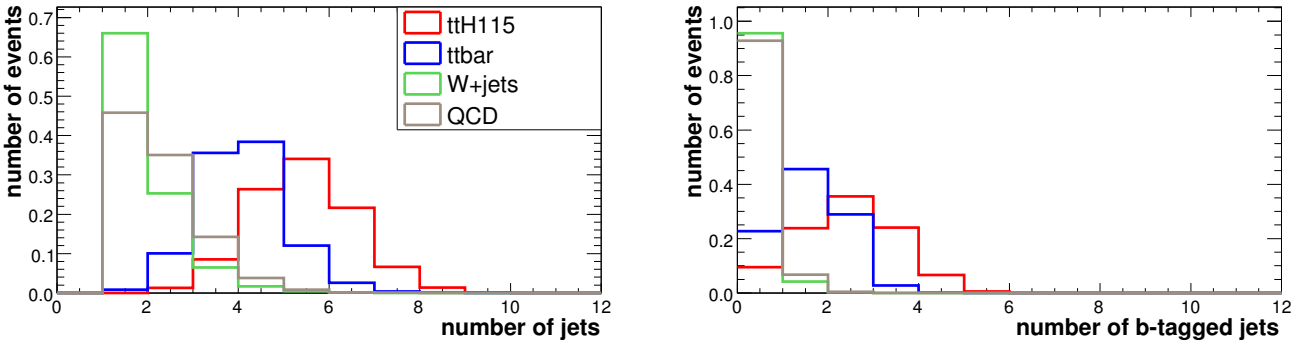

FIG. 2: Normalized distribution of the number of jets (left) and the number of jets which have a NN loose b-tag (right) for $t\bar{t}H$ where the Higgs mass was set to 115 GeV (red), $t\bar{t}$ (blue), W+jets (green) and multijet (brown) production.

was done for both the signal-plus-background and the background-only hypotheses independently by maximizing a profile likelihood function for each hypothesis [5]. The profile likelihood is constructed via a joint Poisson probability over the number of bins in the calculation and is a function of the nuisance parameters in the system and their uncertainties, which are given by an additional Gaussian constraint associated with their prior predictions. Apart from systematics we use the SM $t\bar{t}$ cross section as a nuisance parameter taking the uncertainty as a Gaussian prior. The maximization of the likelihood function is performed over the nuisance parameters.

As a cross-check we studied the background-only hypothesis and found that the $t\bar{t}$ cross section fits at 7.8 pb. This is 0.7σ higher than the SM prediction of 7.29 ± 0.73 pb used as input. Thus we find an agreement with the SM within the uncertainties.

VI. SYSTEMATIC UNCERTAINTIES

The main uncertainties that only change event yields, not the H_T distribution shapes, are due to lepton identification, luminosity, b-tagging [19] and W, $\sigma_{t\bar{t}}$ and $t\bar{t}b\bar{b}$ background models. Another uncertainty on the event preselection is caused by the primary vertex selection and data quality requirements. All of these are summarized in Table 2.

The uncertainties on the jet energy scale and b-tag probabilities for light, c, and b-quark jets are taken as shape dependent uncertainties. We vary these functions, determined from data, by $\pm$ one standard deviation from their central values to find the modifications to the shape of the H_T distributions.

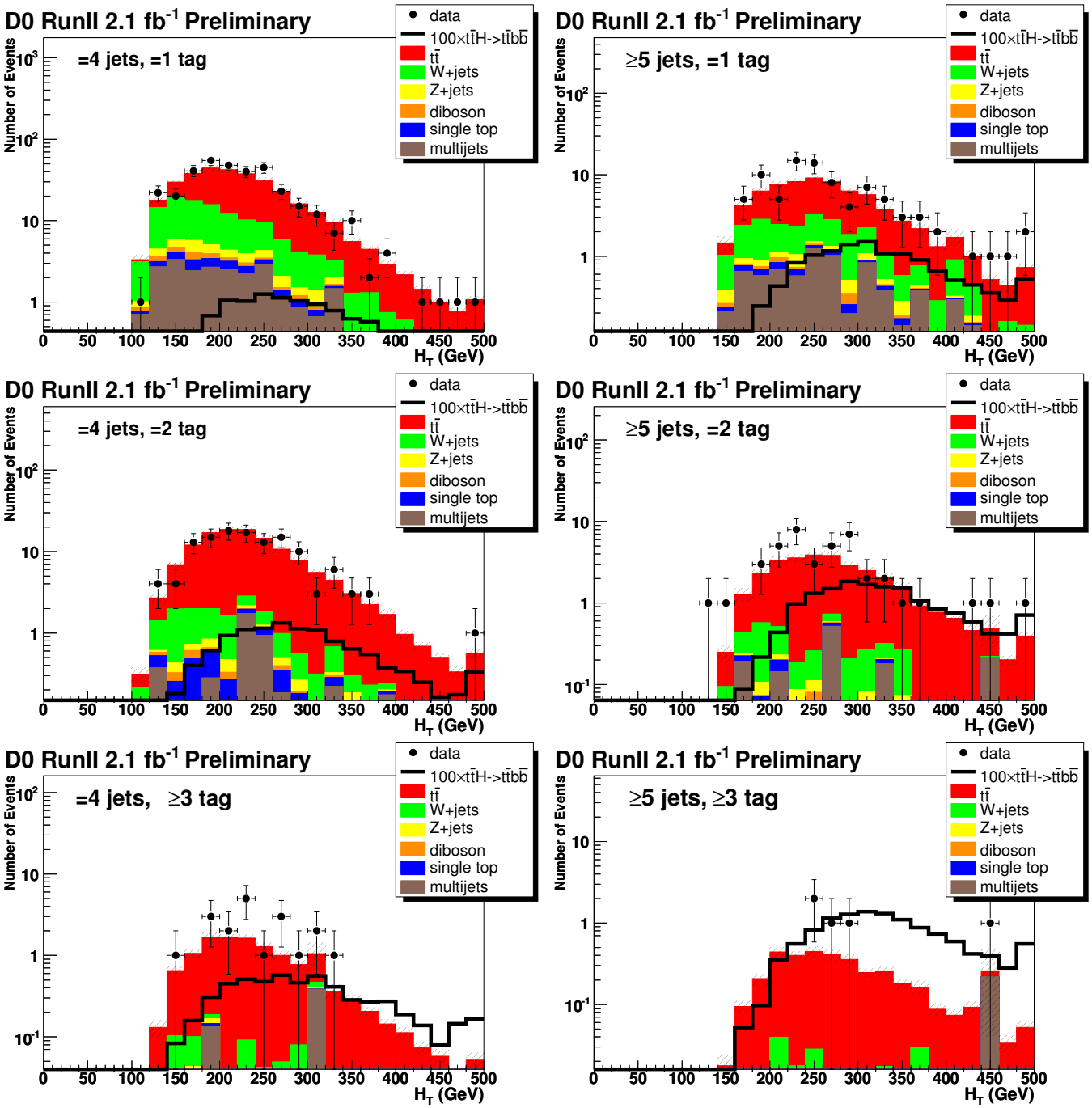

FIG. 3: H_T distributions corresponding to the ℓ+jets data set of 2.1 fb^{-1} requiring 1 b-tag (top row), 2 b-tags (middle row) and ≥ 3 b-tags (bottom row) for events with 4 jets (left column) and ≥ 5 jets (right column). The $t\bar{t}$ cross section is normalized to 7.3 pb corresponding to a top quark mass of 172.6 GeV. The $t\bar{t}H$ signal is for a Higgs mass of 105 GeV and $\sigma(t\bar{t}H) \times B(H \to b\bar{b})$ to 5.5 fb. The signal is enhanced by a factor of 100. The most right bin contains the overflow beyond 500 GeV.

VII. RESULTS

Fig. 4 shows the ratio of the $\sigma_{t\bar{t}H}$ cross section times branching ratio limit over the SM NLO prediction (left plot) and observed and predicted LLR (right plot). The observed limit is in agreement with the expected limit, defined as the median of the limits obtained in background-only pseudo experiments. For a 115 GeV Higgs mass, the observed and expected limits on the $t\bar{t}H$ cross section times branching fraction for $H \to b\bar{b}$ are 45 and 64 times larger than the SM value, respectively. Table 3 gives the numerical values of the expected and observed limits for different Higgs

	e+jets					
	4j1t	4j2t	4j3t	5j1t	5j2t	5j3t
Signal	0.0675	0.0684	0.0318	0.0765	0.0882	0.0669
$t\bar{t}$	110 ± 1	60.5 ± 0.4	5.98 ± 0.12	25.5 ± 0.3	15.0 ± 0.2	1.97 ± 0.07
non-$t\bar{t}$ Bkg	67.2 ± 2.9	8.96 ± 0.97	0.35 ± 0.14	12.9 ± 1.3	2.52 ± 0.62	0.31 ± 0.22
sum Bkg	177 ± 3.0	69.5 ± 1.1	6.32 ± 0.18	38.4 ± 1.4	17.6 ± 0.7	2.28 ± 0.23
Observed	179	57	10	42	22	3
	μ+jets					
	4j1t	4j2t	4j3t	5j1t	5j2t	5j3t
Signal	0.0433	0.0462	0.0237	0.0555	0.0684	0.0504
$t\bar{t}$	91.0 ± 0.5	51.5 ± 0.4	5.04 ± 0.11	20.4 ± 0.2	12.1 ± 0.2	1.47 ± 0.05
non-$t\bar{t}$ Bkg	56.6 ± 2.5	8.5 ± 1.2	0.82 ± 0.44	12.7 ± 1.3	1.84 ± 0.36	0.11 ± 0.10
sum Bkg	148 ± 2.5	60.0 ± 1.2	5.86 ± 0.45	33.2 ± 1.4	14.0 ± 0.4	1.57 ± 0.11
Observed	170	68	9	44	20	2

TABLE 1: Summary of expected and observed yields in the various channels from the 4 jet 1 b-tag bin (4j1t) to the ≥ 5 jet ≥ 3 b-tag bin (5j3t). The expectations are shown for a Higgs mass of 105 GeV. The uncertainties on the signal are about $\pm 0.001 - 0.002$. The background is given for $\sigma_{t\bar{t}} = 7.3$ pb. All uncertainties are statistical only.

Source	value
Event preselection	1.2%
Muon identification	2%
Electron identification	2.5%
Luminosity	6.1%
W background model	15%
Uncertainty on $\sigma_{t\bar{t}}$	10%
Uncertainty on $t\bar{t}b\bar{b}$	50%

TABLE 2: Summary of H_T-independent systematic uncertainties used as input for the limit derivation.

masses.

Higgs mass (GeV)	expected	observed
105	34.3	48.2
115	45.3	63.9
125	64.2	84.8
135	109	151
145	221	291
155	674	835

TABLE 3: Expected and observed ratios of excluded $t\bar{t}H$ cross section times $H \to b\bar{b}$ branching fraction over SM expectation for different values of the Higgs mass.

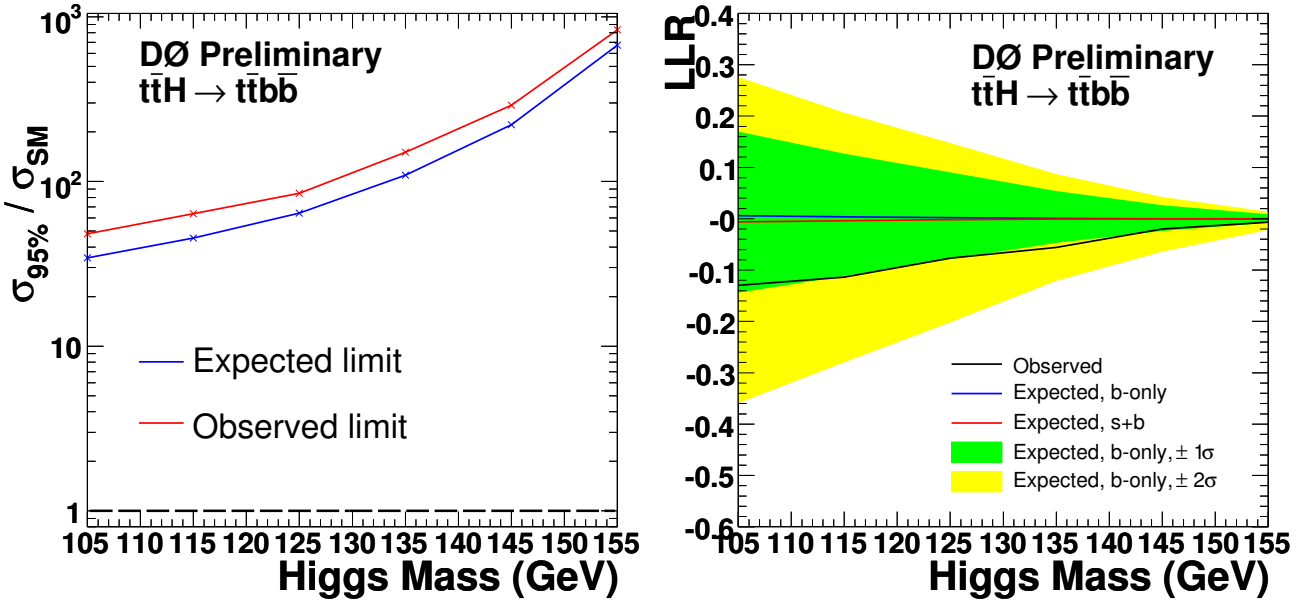

FIG. 4: The 95% CL upper limit on the $\sigma_{t\bar{t}H}$ cross section times branching ratio over the SM expectation in NLO QCD as a function of the Higgs mass (left) and the observed and predicted LLR as a function of the Higgs mass (right).

VIII. SIMULTANEOUS FIT OF $t\bar{t}$ AND $t\bar{t}H$ CROSS SECTIONS

An alternative method where the top quark pair production and the $t\bar{t}H$ cross section are fitted simultaneously is described in this section. For this method we do not use information of the event kinematics but rely on the difference in jet and b-tag multiplicity between signal and background. A sub-dataset of 1 fb^{-1} is used for this study. This corresponds to the full Run-IIa data set.

We split the sample into subsamples with electron or muon, three, four or at least five jets, and zero, one, two or at least three b-tagged jets, resulting in 24 independent data sets. The selection and determination of b-tagging is the same as for the kinematical analysis described in this note. The determination of the signal and all but the W+jets background yield is the same as for the kinematical analysis. For the W+jets background, which is normalized to the data before applying the b-tagging, the yield depends on the $t\bar{t}$ and $t\bar{t}H$ contributions. Therefore the W+jets yield is re-determined iteratively in each step of the fitting procedure used for the measurement of $\sigma_{t\bar{t}}$ and $\sigma_{t\bar{t}H} \times B(H \to b\bar{b})$.

The determination of $\sigma_{t\bar{t}}$ and $\sigma_{t\bar{t}H} \times B(H \to b\bar{b})$ is done with a maximum likelihood fit of the prediction in each subsample to the observed number of events. The likelihood function is defined as the product of Poisson terms for each data set. Additionally Gaussian terms for the systematic uncertainties are multiplied to the likelihood function, with the Gaussian distribution with mean zero and width according to the one sigma value of each source of systematic. With this incorporation of systematic uncertainties the central values of $\sigma_{t\bar{t}}$ and $\sigma_{t\bar{t}H} \times B(H \to b\bar{b})$ can change during the fit.

For several Higgs masses we repeat the fitting procedure and remeasure the $t\bar{t}$ cross section and $\sigma_{t\bar{t}H} \times B(H \to b\bar{b})$. The top quark pair production cross section is found to be consistent

$$\sigma_{t\bar{t}} = 8.36^{+1.08}_{-0.98}\ (\text{stat+syst}) \pm 0.51\ (\text{lumi})\ \text{pb}\quad . \tag{1}$$

This result fluctuates only by 0.01 pb when different Higgs masses are used. As no excess of the data from SM prediction can be observed, limits on $\sigma_{t\bar{t}H} \times B(H \to b\bar{b})$ are set.

The limits on $\sigma_{t\bar{t}H} \times B(H \to b\bar{b})$ are extracted according to the Feldman Cousins procedure [20]. For various input values of $\sigma_{t\bar{t}H} \times B(H \to b\bar{b})$ pseudo-experiments including all systematic uncertainties are generated. Confidence Level bands are built using oderered likelihood ratios. This can be used to extract the 95% C. L. limits at each Higgs mass. The such extracted limits together with the limits on the SM expectation and the 68% error band around the expected limit, divided by the next-to-leading order $\sigma_{t\bar{t}H} \times B(H \to b\bar{b})$ expectation are shown in Fig. 5.

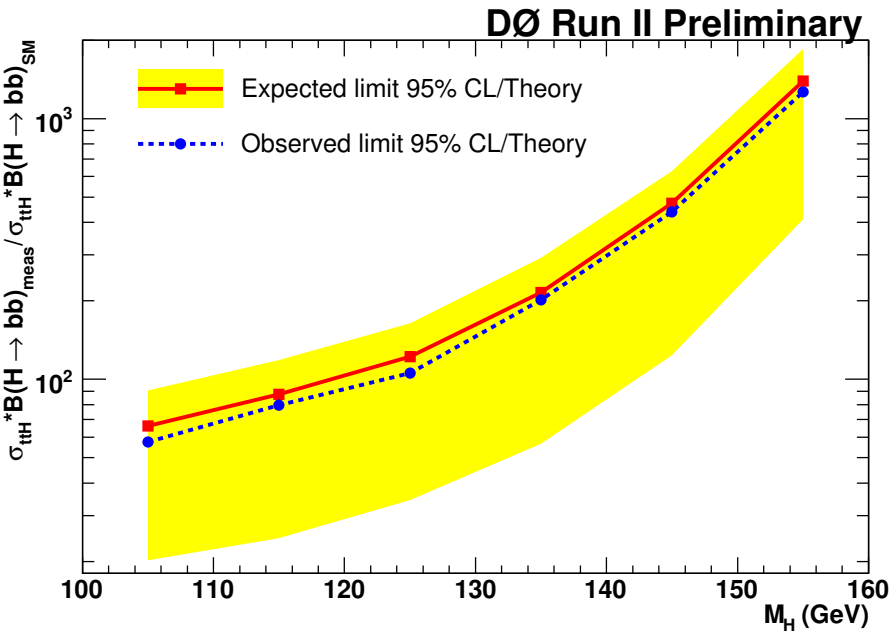

FIG. 5: The 95% CL upper limit on the cross section times branching ratio as a function of the Higgs mass over the SM expectation in NLO QCD for a data set of 1 fb^{-1}. The red line shows the expected limit, the blue one the observed limit. The yellow band gives the total uncertainty on the expected limit.

IX. INTERPRETATION IN A MODEL WHERE t' QUARKS ARE RESONANTLY VIA A HEAVY G' BOSON

Recently, the CDF collaboration performed a search for top-prime (t') quarks and found no evidence for $t'\bar{t}'$ production [21]. In the investigated model t' quarks are pair produced via a SM gluon exchange. In a recent paper [22] it was shown that the t' production cross section at hadron colliders could be substantially higher than the QCD prediction if a "gluon-prime" (G'), i.e. a massive color-octet vector boson, is present in the theory. In such a model a top-prime quark as heavy as 600 GeV can be discovered at the Tevatron. This provides motivation for the search of significantly heavier t' quarks. If the t' originates from a vectorlike quark, then not only $t'\bar{t}'$ production but also the production of a single t' in association with a top may be observable. One possible decay mode of such a single t' into a Higgs boson and a top quark is investigated here (see Fig. 6).

In this section the search for associated Higgs production in top pair events is used to explore such a model that includes both a G' boson and a t' quark. The effect of changes of selection efficiencies due to G' and t' production is assumed to be negligible. This is justified since G' and t' production leads to higher jet and lepton transverse momenta [23]. All signal efficiencies will thus be higher than those assumed in the analyses. Therefore, the limits given in the following are conservative.

The model considered here depends on the t' and G' masses, a mixing angle $\sin\theta_L := s_L$ between the top and t' quark and the coupling strength r. The definitions are given in [22]. The extracted limits depend on the particular choice of those parameters. E.g. the choice $m_{t'} = M_{G'}/2$ maximizes the cross section. For the parameters (r, s_L) chosen here the G' width comes out to be unobservably small. In the considered model there is no b' quark. The parton density function CTEQ6L was used.

Since for the simultaneous fit of $t\bar{t}$ and $t\bar{t}H$ cross sections as described in Section VIII only the difference in jet and b-tag multiplicity between signal and background is investigated, this analysis can be used to search for the following processes:

$$\begin{aligned} p\bar{p} &\to G' \to t\bar{t}' \to t\bar{t}H \to t\bar{t}b\bar{b} \\ p\bar{p} &\to G' \to t'\bar{t} \to t\bar{t}H \to t\bar{t}b\bar{b} \end{aligned} \tag{2}$$

Fig. 6 shows the Feynman graph for the largest contribution to one of the two processes.

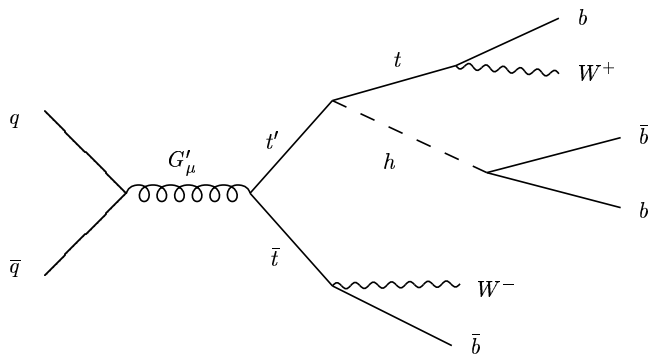

FIG. 6: Feynman graph contributing to Higgs production associated with top pair production via G' exchange as defined in Eq. (2).

Higgs mass (GeV)	cross section (pb), $m_{t'} = 400$ GeV	cross section (pb), $m_{t'} = 450$ GeV	cross section (pb), $m_{t'} = 500$ GeV
105	0.563	0.194	0.0633
115	0.505	0.176	0.0574
125	0.408	0.144	0.0470
135	0.283	0.100	0.0331
145	0.159	0.0575	0.0191
155	0.0624	0.0229	0.00766

TABLE 4: Cross section of processes (2) as a function of the Higgs mass for $m_{t'} = M_{G'}/2$, $r = 0.4$ and $s_L = 0.2$ [22, 23].

The observed limits on $\sigma_{t\bar{t}H} \times B(H \to b\bar{b})$ together with the limits on the SM expectation and the 68% error band around the expected limit are shown in Fig. 7 together with the SM cross section (green dotted). This plot is the same as Fig. 5 except that it was not divided by the SM cross section. Neglecting differences in the selection efficiencies between SM $t\bar{t}H$ production and the production via G' exchange one can include the theoretical cross section as a function of the Higgs mass as given in Tab. 4 into the excluded cross section limit of Fig. 7 for different values of the $t' = M_{G'}/2$ mass (black solid, dashed and fine dashed).

Comparing the observed cross section limit to the $t\bar{t}H$ production cross section via G' exchange excludes, for example, $M_H < 133$ GeV for $m_{t'} = 400$ GeV and $M_{G'} = 800$ GeV at 95% CL. The excluded region as a function of the Higgs mass and the t' mass is shown in Fig. 8.

X. SUMMARY

We performed a search for the production cross section of the SM Higgs boson in association with top and antitop quarks in a data set of 2.1 fb^{-1}. We analyzed kinematical information using the H_T distributions in different bins of jets multiplicity and b-tagged jets multiplicity. The channels with 4 or ≥ 5 jets and ≥ 3 b-tags were investigated separately for the first time. In all channels within the uncertainties we found agreement between the observed and expected number of events. No hint of associated Higgs production or any other type of physics beyond the SM was found.

We derive upper limits on $t\bar{t}H$ production. They strongly depend on the mass of the Higgs boson. For low masses around 115 GeV the expected limit for $\sigma(t\bar{t}H) \times B(H \to b\bar{b})$ is 45 times larger than the SM prediction. The observed limit is a factor of 64 larger than the SM calculation.

Furthermore, it has been shown that the search for $t\bar{t}H$ production provides valuable information about models that predict t' quarks produced via a heavy G' boson exchange.

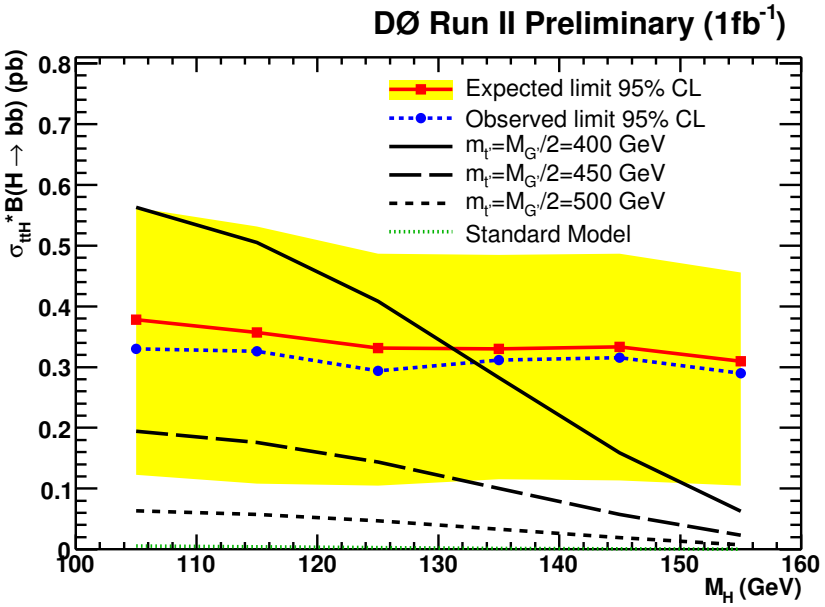

FIG. 7: The 95% CL upper limit on the cross section times SM branching ratio Br($H \to b\bar{b}$) as a function of the SM Higgs mass for a data set of 1 fb^{-1}. The red line shows the expected limit, the blue one the observed limit. The yellow band gives the total uncertainty on the expected limit. The green curve gives the SM expectation in NLO QCD. The theoretical calculation of processes (2) as given in Tab. 4 is shown for three different values of $m_{t'} = M_{G'}/2$ and for $r = 0.4$ and $s_L = 0.2$.

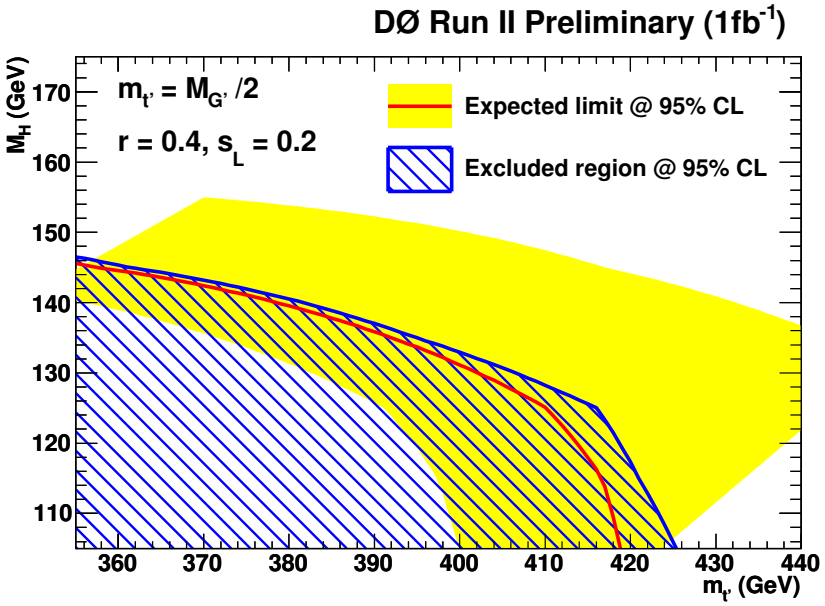

FIG. 8: Excluded region at 95% CL as a function of the Higgs mass and the t' mass for a data set of 1 fb^{-1}. The red line shows the expected limit, the blue one the observed limit. For the theoretical cross section of processes (2) $m_{t'} = M_{G'}/2$, $r = 0.4$ and $s_L = 0.2$ is assumed.

Acknowledgments

We are grateful to B. A. Dobrescu, K. Kong and R. Mahbubani for many fruitful and interesting discussions about this exciting topic and providing us with additional calculations.

We thank the staffs at Fermilab and collaborating institutions, and acknowledge support from the Department of Energy and National Science Foundation (USA), Commissariat à l'Energie Atomique and CNRS/Institut National de Physique Nucléaire et de Physique des Particules (France), Ministry of Education and Science, Agency for Atomic Energy and RF President Grants Program (Russia), CAPES, CNPq, FAPERJ, FAPESP and FUNDUNESP (Brazil), Departments of Atomic Energy and Science and Technology (India), Colciencias (Colombia), CONACyT (Mexico), KRF (Korea), CONICET and UBACyT (Argentina), The Foundation for Fundamental Research on Matter (The Netherlands), PPARC (United Kingdom), Ministry of Education (Czech Republic), Natural Sciences and Engineering Research Council and WestGrid Project (Canada), BMBF (Germany), A.P. Sloan Foundation, Civilian Research and Development Foundation, Research Corporation, Texas Advanced Research Program, and the Alexander von Humboldt Foundation.

[1] [CDF, D0 Collaborations], arXiv:0803.1683 [hep-ex].
[2] A. Stange and S. Willenbrock, Phys. Rev. D **48**, 2054 (1993) [arXiv:hep-ph/9302291].
[3] T. F. Feng, X. Q. Li and J. Maalampi, Phys. Rev. D **69**, 115007 (2004) [arXiv:hep-ph/0310247].
[4] J. A. Aguilar-Saavedra, JHEP **0612**, 033 (2006) [arXiv:hep-ph/0603200].
[5] W. Fisher, FERMILAB-TM-2386-E.
[6] The DØ Collaboration, DØ note 5715-CONF.
[7] V. M. Abazov *et al.* [D0 Collaboration], "The upgraded D0 detector," Nucl. Instrum. Meth. A **565**, 463 (2006) [arXiv:physics/0507191].
[8] Rapidity y and pseudorapidity η are defined as functions of the polar angle θ and parameter β as $y(\theta,\beta) \equiv \frac{1}{2}\ln\left[(1+\beta\cos\theta)/(1-\beta\cos\theta)\right]$ and $\eta(\theta) \equiv y(\theta,1)$, where β is the ratio of a particle's momentum to its energy.
[9] Impact parameter is defined as the distance of closest approach (d_{ca}) of the track to the primary vertex in the plane transverse to the beamline. Impact parameter significance is defined as $d_{ca}/\sigma_{d_{ca}}$, where $\sigma_{d_{ca}}$ is the uncertainty on d_{ca}.
[10] V. M. Abazov *et al.*, Nucl. Instrum. Meth. A **552**, 372 (2005) [arXiv:physics/0503151].
[11] V.M. Abazov *et al.*, (DØ Collaboration), Phys. Rev. Lett. **100**, 192003 (2008).
[12] The DØ Collaboration, DØ note 5610-CONF.
[13] T. Sjöstrand, L. Lönnblad, S. Mrenna, hep-ph/0308153 (2003).
[14] J. Pumplin et al., JHEP 0207, 012(2002).
[15] M. L. Mangano et al, CERN-TH-2002-129, FTN-T-2002-06, hep-ph/0206293 (2002).
[16] N. Kidonakis and R. Vogt, Phys. Rev. D **68**, 114014 (2003).
[17] M. Cacciari *et al.*, hep-ph/0303085 (2003).
[18] T. Junk, Nucl. Instrum. Methods in Phys. Res. A **434**, 435 (1999); A. Read, in *"1st Workshop on Confidence Limits,"* CERN Report No. CERN-2000-005, 2000.
[19] T. Scanlon, FERMILAB-THESIS-2006-43.
[20] G. Feldman, R. Cousins, Phys. Rev. D 57, 3873 (1998)
[21] T. Aaltonen *et al.* [CDF Collaboration], Phys. Rev. Lett. **100**, 161803 (2008) [arXiv:0801.3877 [hep-ex]]; The CDF Collaboration, Conference Note 9446.
[22] B. A. Dobrescu, K. Kong and R. Mahbubani, "Prospects for top-prime quark discovery at the Tevatron," arXiv:0902.0792 [hep-ph].
[23] B. A. Dobrescu, K. Kong and R. Mahbubani, private communication.

APPENDIX A: EVENT DISPLAY

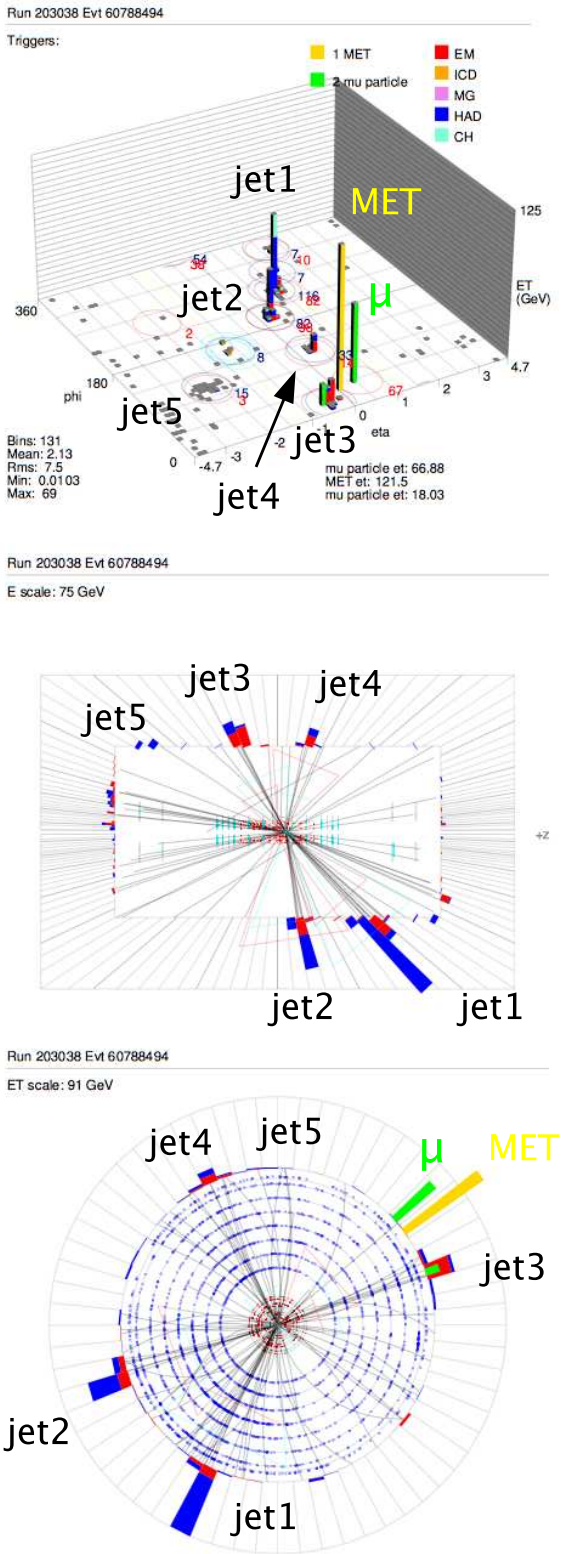

FIG. 9: Example μ+jet event with 3 b-tags and 5 jets. Jet1, jet2 and jet3 have a b-tag. The transverse momenta of the objects in the final state are $p_T^{\rm jet1}$=156 GeV, $p_T^{\rm jet2}$=111 GeV, $p_T^{\rm jet3}$=104 GeV, $p_T^{\rm jet4}$=49 GeV, $p_T^{\rm jet5}$=24 GeV, p_T^{μ}=67 GeV. $\not\!\!E_T$=50 GeV. H_T=444 GeV.